

# A constitutive model for dynamic plasticity of FCC metals

C.Y. Gao<sup>a</sup>, L.C. Zhang<sup>b,\*</sup>

<sup>a</sup> Department of Mechanics, Zhejiang University, Hangzhou, 310027, China

<sup>b</sup> School of Mechanical and Manufacturing Engineering, The University of New South Wales, Sydney, NSW 2052, Australia

## ARTICLE INFO

### Article history:

Received 6 January 2010

Received in revised form 19 January 2010

Accepted 22 January 2010

### Keywords:

Constitutive relation  
Plastic deformation  
Dislocation mechanisms  
OFHC copper  
High strain rate  
Large strain

## ABSTRACT

This paper proposes a new constitutive model to describe the dynamic plasticity of FCC metals using the thermal activation mechanism of dislocation motion. In the model development, the constitutive parameters were directly linked with the characteristics of microstructures of materials. As an example of its application, the model was used to describe the behavior of OFHC copper. To determine the globally optimized parameters of the constitutive model for OFHC copper, an improved multi-variable optimization method of constrained nonlinear programming was used based on the flow stress of the material measured experimentally. A comparison with some models and experimental data in the literature shows that the new model is simple to apply and is much better in terms of its prediction accuracy. It was shown that compared with the MTS model the new constitutive equation is explicit and can be easily embedded into a computational code of material dynamics; while compared with the Zerilli–Armstrong and Johnson–Cook models the new one reflects more precisely experimental observations. It was concluded that the new model is applicable to a wide range of problems with temperature variation from 77 K to 1096 K, strain rates ranging from  $10^{-3} \text{ s}^{-1}$  to  $10^4 \text{ s}^{-1}$ , and strain as high as 1.

© 2010 Elsevier B.V. All rights reserved.

## 1. Introduction

A reliable constitutive model is necessary to describe properly the dynamic response of a material under a deformation with large temperature variation, high strain rate and large strain. Such constitutive models must have the ability to reflect the complicated relationships among the main mechanical state variables of a material. In general, the dynamic yield stress of a material can be described by a function of some state variables such as plastic strain, strain rate, temperature, and some structural parameters related to deformation history. Over the past decades, quite some empirical constitutive models have been proposed based on the conventional phenomenological theory, of which the Johnson–Cook model, or called the J–C equation, is the most widely used [1]. It has been reported that the J–C equation can successfully describe the experimental results of the well-known Taylor cylinder impact test, and is convenient to use because the essential parameters of a variety of materials required by this constitutive equation can be obtained relatively easily. However, it has also been reported that the J–C equation cannot describe or represent many experimental observations/measurements, particularly when a material is subjected to a high strain rate, such as under high speed machining [2]. This is because the dynamic behavior of a material at high strain rates

is closely related to the microstructural evolution of the material during deformation, which is not included in a conventional phenomenological constitutive equation. A physical constitutive model is therefore necessary.

Dislocation dynamics has been used in constitutive modelling since the 1960s. For example, Campbell and Harding [3] studied the dynamic response of low-carbon steels at high strain rates through a thermal activation analysis of dislocation motion. Frost and Ashby [4] deduced various rate-dependent constitutive equations for dislocation motions in the plastic deformation of materials. They then described the regimes of deformation mechanisms relative to various strain rates and temperature variations. Zerilli and Armstrong proposed a constitutive relation using a thermal activation analysis [5]. They found that the dislocation mechanisms in metals of different crystalline structures were different. For face-centered cubic (FCC) metals, dislocations must traverse the barriers of forest dislocations, and the thermal activation area decreases with plastic strain because of the increase in dislocation density. Nevertheless, for body-centered cubic (BCC) metals, dislocations must overcome Peierls–Nabarro barriers (i.e. Peierls internal stress), and thus the thermal activation area is not related with strain. Hence, the yield stress of FCC metals is determined mainly by strain hardening, but that of BCC metals is basically determined by strain rate hardening and temperature softening. Based on these considerations, Zerilli and Armstrong proposed different constitutive relations for FCC and BCC metals. It was claimed that the Zerilli–Armstrong model can describe the behavior of metals with a hexagonal close-packed (HCP) crystalline structure, because HCP has the partial structural

\* Corresponding author. Tel.: +61 2 9385 6078; fax: +61 2 9385 7316.

E-mail addresses: [lxgao@zju.edu.cn](mailto:lxgao@zju.edu.cn) (C.Y. Gao), [Liangchi.Zhang@unsw.edu.au](mailto:Liangchi.Zhang@unsw.edu.au) (L.C. Zhang).

**Nomenclature**

$b$	Burgers vector
$c_3$	$=k/(g_{s0}\mu b^3)$
$c_4$	$=k/(g_0\mu b^3)$
$c_p$	specific heat of materials
$d$	the diameter of grain
$f$	the influencing factor (<1) of strain rate and temperature effects
$F(X)$	denoting a function relationship, where $X = \hat{\sigma}_{th}/\hat{\sigma}_{th,s}$
$g_0$	normalized free energy
$g_{s0}$	saturated normalized free energy
$G_0$	reference free energy
$k$	Boltzmann constant
$\tilde{k}$	the microstructural stress modulus
$m'$	Schmidt factor
$n$	$=n_2/n_1$
$p, q$	a pair of parameters representing the shape of crystal potential barrier
$T$	temperature
$T_0$	initial temperature
$v$	dislocation velocity
$v_0$	reference limit dislocation velocity
$\dot{Y}$	$=\lambda\hat{\sigma}_{s0}$

*Greek letters*

$\Delta G$	free energy of thermal activation
$\lambda_1, n_1$	material constants
$\lambda_2, n_2$	material constants
$\lambda$	$=(\lambda_2/\lambda_1)^{1/n_1}$
$\sigma$	flow stress
$\sigma_a$	athermal stress
$\sigma_{th}$	thermal stress
$\hat{\sigma}$	mechanical threshold stress (MTS)
$\hat{\sigma}_a$	athermal component of MTS
$\hat{\sigma}_{th}$	thermal component of MTS
$\hat{\sigma}_s$	saturated threshold stress
$\hat{\sigma}_{s0}$	reference saturated threshold stress
$\hat{\sigma}_{th,s}$	thermal component of $\hat{\sigma}_s$
$\sigma_G$	the stress brought by initial defects
$\varepsilon$	plastic (true) strain
$\dot{\varepsilon}$	plastic strain rate
$\dot{\varepsilon}_0$	reference strain rate
$\dot{\varepsilon}_{s0}$	saturated reference strain rate
$\mu$	shear modulus
$\rho$	material's density
$\rho_m$	moving dislocation density
$\theta$	strain hardening rate
$\theta_0$	hardening rate due to dislocation accumulation
$\theta_\tau$	dynamic recovery rate
$\eta$	the converting efficiency from plastic work to dissipated heat

characteristics of BCC and FCC. However, Voyiadjis and Abed [6] pointed out that the Zerilli–Armstrong model is not applicable to the deformation of metals under high temperature because of an approximation in its formulation and because the strain rate effect on thermal activation area has not been considered. Voyiadjis and Abed then proposed an improved model [7]. Nemat-Nasser and Li [8] introduced a variable reference strain rate, as a function of strain and temperature, and obtained a model applicable to both FCC and BCC metals [9,10].

Follansbee and Kocks developed a constitutive model for copper using the concept of mechanical threshold stress (MTS) [11–13]. They found in their experiment that the strain rate sensitivity of flow stress of pure copper dramatically increases when strain rate approaches  $10^4 \text{ s}^{-1}$ . They explained that this was due to the dependence of strain hardening rate on strain rate. A disadvantage of the Follansbee–Kocks model is that the MTS representing the structural evolution cannot be expressed as an explicit function of strain, leading to a complex equation which is not so straightforward for application. There are many similar works on the constitutive modelling of dynamic deformation involving physical mechanisms [14–17] and microstructural evolution [18,19], but their applicability was limited.

This paper will develop a new physical constitutive model for FCC metals. Section 2 of the paper will formulate our new constitutive model based on the theory of thermal activation mechanism of dislocation motion, where the physical meaning of each constitutive parameter will be shown by their relationships with microstructural characteristics. Section 3 of the paper will describe the method to determine the optimal constitutive parameters for oxygen-free high conductivity (OFHC) copper. Section 4 will compare the model with experimental data and some representative models in the literature. Finally, Section 5 will summarize the main advantages of the new model.

**2. Physical constitutive formulation of FCC metals**

The plastic deformation of metals can be explained as the process of dislocation motion and accumulation with the rate-controlled deformation mechanism. The physical constitutive models of metals have been developed based on the notion of thermally activated dislocation kinetics for moderate strain rates less than  $10^4 \text{ s}^{-1}$ , and on the notion of the dislocation-drag deformation mechanism for greater strain rates [8]. In the thermal activation analysis, plastic flow is mainly controlled by the motion of dislocations which is opposed by both short-range and long-range obstacles. The short-range barriers may be overcome by thermal activation, whereas the long-range barriers are essentially independent of the temperature (i.e. it is athermal). The short-range barriers may include forest dislocations (i.e., the intersection of dislocation forests, which is the principal mechanism in FCC metals [5]), Peierls stress (i.e., the overcoming of Peierls–Nabarro barriers, which is the principal mechanism in BCC metals), point defects (e.g., vacancies and self-interstitials), alloy elements, solute atoms (interstitials and substitutionals), impurities, deposits and so on. The long-range barriers may include grain boundaries, far-field dislocation forests, and other microstructural elements with far-field influence. Therefore, the flow stress of the materials, which is essentially defined by the material resistance to dislocation motion, can be correspondingly decomposed into

$$\sigma = \sigma_a + \sigma_{th} \quad (1)$$

where  $\sigma_a$  is the athermal component of the flow stress reflecting the long-range barriers and is independent of the thermal activation, while  $\sigma_{th}$  is the thermal component of the flow stress reflecting the short-range barriers but depends on the thermal activation. Similarly, the MTS (the flow stress at 0 K, denoted as  $\hat{\sigma}$ ) can be decomposed as the sum of the athermal and thermal components,  $\hat{\sigma} = \hat{\sigma}_a + \hat{\sigma}_{th}$ . As there is no thermal activation energy at 0 K, the height of the short-range barriers is maximal. This height will fall when temperature increases due to the increase of the atom vibration amplitude activated by the thermal energy, which helps a dislocation to overcome barriers. Accordingly, the thermal stress will decrease while the athermal stress remains unchanged. If the MTS is regarded as a reference stress that characterizes the struc-

ture of a metal, the flow stress of the material can be expressed as

$$\sigma = \hat{\sigma}_a + f(\dot{\varepsilon}, T)\hat{\sigma}_{th} \quad (2)$$

where  $\hat{\sigma}_a$  is the athermal component,  $f(\dot{\varepsilon}, T)$  is the influencing factor ( $<1$ ) representing the strain rate and temperature effects, and  $\hat{\sigma}_{th}$  is the threshold thermal stress related to the material's microstructure and structural evolution. If the effect of grain size is considered based on the Hall–Petch relationship, then

$$\hat{\sigma}_a = \sigma_G + \tilde{k}d^{-1/2} \quad (3)$$

where  $\sigma_G$  is the stress due to initial defects,  $d$  is the diameter of the grain and  $\tilde{k}$  is a microstructural stress modulus. The athermal component could be regarded as constant if there is no physical change (such as twinning) to alter the average grain size during plastic deformation. In fact, the grain size effect is relatively small for conventional course-grained materials. More discussion about the importance of the grain size effect, especially for nanocrystalline materials, can be found in Refs. [20–22].

In the following part, we will focus on how to determine two key internal state variables  $f$  and  $\hat{\sigma}_{th}$  in Eq. (2).

### 2.1. Thermal activation analysis at constant structure

The motion of a dislocation in metals is driven by the plastic flow stress caused by the external force of dynamic loading. Then, as Orowan [23] pointed out, there should be a relationship between the plastic strain rate and the average dislocation velocity,

$$\dot{\varepsilon} = m'b\rho_m v \quad (4)$$

where  $m'$  is the Schmidt factor,  $b$  is the Burgers vector representing the excursion induced by dislocation and  $\rho_m$  is the moving dislocation density. On the other hand, Johnston and Gilman [24] obtained the following relation:

$$v = v_0 \exp\left(\frac{-\Delta G(\sigma)}{kT}\right) \quad (5)$$

from their experimental and theoretic analysis, where  $v_0$  is the reference limit dislocation velocity,  $k$  is the Boltzmann constant,  $T$  is the absolute temperature, and  $\Delta G$  is the free energy of thermal activation (Gibbs free energy), which is a stress function related to the barrier shape (such as the rectangular, square, triangular, parabolic and exponential ones). Kocks and Ashby [25] proposed the following generalized equation with two parameters to fit any shapes:

$$\Delta G = G_0 \left(1 - \left(\frac{\sigma_{th}}{\hat{\sigma}_{th}}\right)^p\right)^q \quad (6)$$

where  $G_0$  is the reference free energy at 0 K ( $=g_0\mu b^3$ ),  $g_0$  is a normalized free energy and  $\mu$  is the shear modulus),  $p$  and  $q$  are a pair of parameters representing the shape of crystal potential barrier (e.g., the values of [2/3,1] mean a rectangular barrier). In the equation, the current structure has been considered as constant in the thermal activation analysis. Hence, if combining Eqs. (4)–(6) and considering Eq. (2), we obtain

$$f(\dot{\varepsilon}, T) = \left\{1 - \left[-\left(\frac{kT}{G_0}\right) \ln\left(\frac{\dot{\varepsilon}}{\dot{\varepsilon}_0}\right)\right]^{1/q}\right\}^{1/p} \quad (7)$$

where  $\dot{\varepsilon}_0 = m'b\rho_m v_0$  is defined as the reference strain rate. Thus,  $f$  is obtained at the condition of a constant structure.

### 2.2. Structural evolution

In reality, a structure will evolve with strain under the influence of strain rate and temperature, and the evolution process is the

result of the balance between two competing processes, dislocation accumulation and dynamic recovery. The deformation history effect is also reflected in the evolution. The strain hardening rate can be defined by:

$$\theta = \frac{d\hat{\sigma}}{d\varepsilon} = \theta_0 - \theta_\tau(\dot{\varepsilon}, T, \hat{\sigma}) \quad (8)$$

where  $\theta_0$  is the hardening rate due to dislocation accumulation,  $\theta_\tau$  is dynamic recovery rate in which  $\hat{\sigma}$  represents the characteristics of a material structure. Assuming that the strain hardening does saturate and the strain range is below 1.0, we can have the following strain hardening description:

$$\theta = \theta_0[1 - F(X)] \quad (9)$$

where  $F$  denotes a function relationship and  $X = \hat{\sigma}_{th}/\hat{\sigma}_{th,s}$ .  $\hat{\sigma}_{th,s}$  is the thermal threshold stress in the saturated state (i.e.,  $\theta = 0$ ) which includes the influences of strain rate and temperature on structural evolution. For a simple linear relationship of strain hardening, i.e., if  $F(X) = X$ , the strain hardening by Eq. (9) becomes the well-known Voce behavior. Kocks, et al [11] proposed a hyperbolic tangent function for  $F(X)$  by trial and error using some  $\theta \sim \hat{\sigma}$  curves. This is merely a mathematical fitting to the experiment data without physical considerations. However, we know that the true  $\theta \sim X$  relation must vary with strain rate and temperature, and that the strain hardening rate should become zero when the flow stress reaches its saturation. Based on these considerations, we found that a power function is actually a better approximation to the true relation, because it is simpler and reflects the saturation status more reasonably. The linear Voce relation is too simple to describe properly the strain hardening rate, and the hyperbolic tangent function is unnecessarily complex because it does not allow an explicit description between the threshold thermal stress and strain after integration, and makes the constitutive model difficult to use. We notice that a power function can effectively describe the strain hardening behavior, and is a good approximation to the hyperbolic tangent function if the constant parameters in the function are carefully selected. Based on this consideration, we propose the following power law relation:

$$F(X) = \lambda_1 X^{n_1} \quad (10)$$

where  $\lambda_1$  and  $n_1$  are constants. By combining Eq. (10) with Eq. (9), we know that the relation of  $\theta \sim \hat{\sigma}$  follows a power law.

On the other hand, we find from the relation curves of  $\theta \sim \varepsilon$  and  $\theta \sim \hat{\sigma}$  in [11] that the two relations should have the same functional form (but with different concavity factors). That is to say, the relation curve of  $\theta \sim \varepsilon$  should follow a power law too, as verified in [26]. Then

$$\theta = \theta_0[1 - \lambda_2 \varepsilon^{n_2}] \quad (11)$$

where  $\lambda_2$  and  $n_2$  are constants. Now, comparing Eq. (9) with Eq. (11), we can obtain the following relation:

$$\hat{\sigma}_{th} = \lambda \hat{\sigma}_{th,s} \varepsilon^n \quad (12)$$

where  $\lambda = (\lambda_2/\lambda_1)^{1/n_1}$  and  $n = n_2/n_1$  are material constants. Davis proved the single curve assumption by experimental results [27]. On the basis of this assumption, the relation of equivalent stress and strain can be approximated by the relation of uniaxial stress and strain under simple or approximately simple loading conditions. At the same time, the relation of uniaxial stress and strain can be determined by uniaxial loading test and is found to be able to be described very well by the power law. Thus, a power law relationship between  $\hat{\sigma}_{th}$  and  $\varepsilon$  described by Eq. (12) is reasonable.

In addition, when strain hardening decreases with dynamic recovery until the last saturated state, the saturated value of the

**Table 1**  
Determined constitutive parameters for OFHC copper.

Constitutive parameters	Units adopted	Determined values	Theoretically estimated range
$\hat{\sigma}_a$	MPa	70.6	(0, 100)
$\hat{Y}$	MPa	808	(500, 1000)
$c_3$	1/K	$1.0 \times 10^{-5}$	$(1.0 \times 10^{-5}, 1.0 \times 10^{-4})$
$c_4$	1/K	$5.43 \times 10^{-5}$	$(1.0 \times 10^{-5}, 1.0 \times 10^{-4})$
$p$	–	2/3	(0, 1]
$q$	–	1.0	[1,2]

threshold stress,  $\hat{\sigma}_s$ , can be described by [11]

$$\ln\left(\frac{\dot{\epsilon}}{\dot{\epsilon}_{s0}}\right) = \left(\frac{g_{s0}\mu b^3}{kT}\right) \ln\left(\frac{\hat{\sigma}_s}{\hat{\sigma}_{s0}}\right) \quad (13)$$

where  $\dot{\epsilon}_{s0}$  is the saturated reference strain rate,  $\hat{\sigma}_{s0}$  is the reference saturated threshold stress and  $g_{s0}$  is a constant. Because the athermal component of saturated threshold stress occupies a small proportion,  $\hat{\sigma}_s \approx \hat{\sigma}_{th,s}$ . By introducing this approximation into Eq. (12) and combining it with Eq. (13), we get

$$\hat{\sigma}_{th} = \lambda \hat{\sigma}_{s0} \epsilon^n \exp\left[\left(\frac{kT}{g_{s0}\mu b^3}\right) \ln\left(\frac{\dot{\epsilon}}{\dot{\epsilon}_{s0}}\right)\right] \quad (14)$$

Finally, by substituting Eqs. (7) and (14) into Eq. (2), we obtain our new constitutive relation as follows:

$$\sigma = \hat{\sigma}_a + \hat{Y} \epsilon^n \exp\left[c_3 T \ln\left(\frac{\dot{\epsilon}}{\dot{\epsilon}_{s0}}\right)\right] \left\{1 - \left[-c_4 T \ln\left(\frac{\dot{\epsilon}}{\dot{\epsilon}_0}\right)\right]^{1/q}\right\}^{1/p} \quad (15)$$

where  $\hat{Y} (= \lambda \hat{\sigma}_{s0})$  is the actual reference thermal stress,  $c_3 = k/(g_{s0}\mu b^3)$  and  $c_4 = k/(g_0\mu b^3)$ .

The constitutive equation developed above is one-dimensional corresponding to the experimental data of uniaxial loading. However, it can be transformed into the tensor form of three-dimensional cases [28] when the flow stress is replaced by the von Mises stress.

If a localized adiabatic shear at high strain rates happens, or in other words, if an adiabatic process occurs, the majority of the plastic work is converted to the internal dissipation heat in materials, and will cause a local rapid increase of temperature. The increased temperature can be calculated as

$$T = T_0 + \frac{\eta}{\rho c_p} \int_0^\epsilon \sigma d\epsilon \quad (16)$$

where  $\rho$  is the material's density,  $c_p$  is the material's specific heat at constant pressure, and  $\eta$  is the converting efficiency from plastic work to heat (also called the Taylor–Quinney empirical constant, ranging generally between 0.9 and 1.0). Thus, in the calculation of the flow stress by using the constitutive relation above, Eq. (15), the state variable of temperature should be updated instantly at each strain step.

### 3. Determination of constitutive parameters for OFHC copper

In the following, we describe the method to determine the parameters of our new constitutive equation, Eq. (15), for a typical FCC metal, the fully annealed polycrystalline OFHC copper of high purity (>0.9999).

It is well known that for FCC metals, the thermal stress is basically proportional to the square root of strain [5]. Hence,  $n = 1/2$ . This also shows the rationality of our power-function form of strain which is assumed for strain hardening rate in the deduction of the constitutive relation in Section 2. Although  $n = 1/2$  is not very precise for all FCC metals, the error is small (<6%) [6].

Parameters  $\dot{\epsilon}_{s0}$  and  $\dot{\epsilon}_0$  are in the logarithmic functions. The influence of their value changes, relative to that of  $c_3$  and  $c_4$ , is small. Furthermore, they are dependent on  $c_3$  and  $c_4$ . Hence, if  $\dot{\epsilon}_{s0}$  and  $\dot{\epsilon}_0$  can be evaluated before the determination of  $c_3$  and  $c_4$ , the errors in evaluating  $\dot{\epsilon}_{s0}$  and  $\dot{\epsilon}_0$  can be offset by the fitting of  $c_3$  and  $c_4$ . In doing so, we not only avoid the problem of discrete valuations to the two parameters in the literature [5,7,8,11], but also enhance the robustness of the nonlinear optimization algorithm used in determining the other parameters (i.e.,  $\hat{\sigma}_a, \hat{Y}, c_3, c_4, p, q$ ). The value of  $\dot{\epsilon}_{s0}$  is found to be  $3.75 \times 10^{10} s^{-1}$  from the Zerilli–Armstrong model of OFHC copper, and that of  $\dot{\epsilon}_0$  is  $1.76 \times 10^8 s^{-1}$  from the Voyiadjis–Abed model of OFHC copper.

The remaining six parameters,  $\hat{\sigma}_a, \hat{Y}, c_3, c_4, p, q$ , can be determined by using the experimental data. For example, we can use a group of stress–strain curves measured at different temperatures and a given strain rate of 4000/s for OFHC copper [8]. To determine an optimized group of these parameters, the multi-variable constrained nonlinear programming on the basis of the least square principle was used with the aid of the optimization tool in Matlab. To do so, the sequential quadratic programming (SQP) method [29] was selected to maximize the precision of the results. Table 1 below lists the optimized results of the constitutive parameters.

### 4. Results, discussion and experimental validation

In the following results, all the theoretical predictions of flow stress are adiabatic except the case of very low strain rate, and hence the temperature indicated is only initial temperature.

Fig. 1 compares the flow stress predictions of our new model with the experimental data. It can be seen that the model describes well the flow stress of the material within a broad temperature range at high strain rates, especially in the case of high temperature that the Zerilli–Armstrong model does not apply. Our new constitutive model shows that the adiabatic shear effect is not obvious at a strain below 0.8 (the induced error is less than 10%).

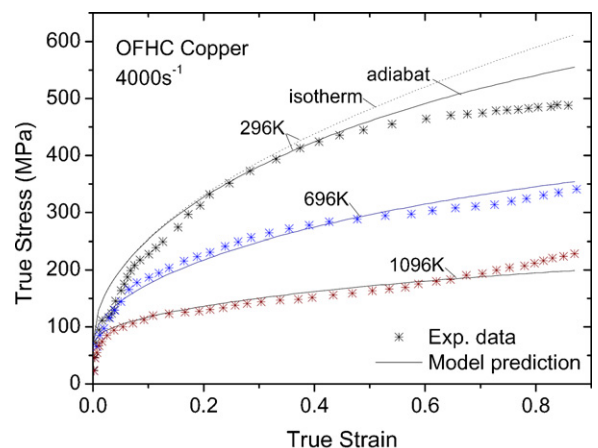


**Fig. 1.** Comparison of our model prediction with the experimental data [8] for annealed OFHC copper at different temperatures with the strain rate of 4000/s.

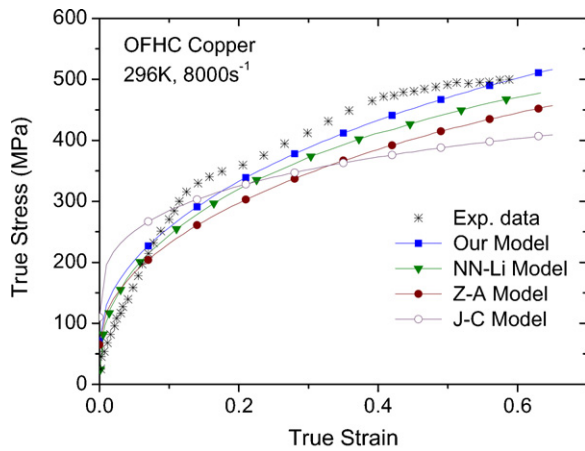


Fig. 2. Comparison of the predictions by different models with experimental data [8] for annealed OFHC copper at 296 K with the strain rate of 8000/s.

Fig. 2 compares the new model with some common constitutive models in the literature at 296 K and 8000/s based on the experimental results of Nemat-Nasser and Li. It can be seen that the prediction of the new model is better than all the others. The J-C model shows less accuracy, reached an error of 20% at the strain of 0.6.

If our new model can better represent the constitutive physics of the material deformation, it should predict more reasonably a wide range of strain rates than the other models in the literature, even though the constitutive parameters of our model were determined using a set of limited experimental data at a specific strain rate (4000/s). To examine this, two case studies were carried out and are described below. One is a case of a very low strain rate and the other is with a very high strain rate.

Fig. 3 shows the predictions and experimental results at 296 K and 0.001/s. It is obvious that our model can better describe the quasi-static plastic deformation, because plastic deformation at low strain rates and room temperature is still controlled by the thermal activation mechanism.

Fig. 4 compares the predictions with Clifton's experimental results at 296 K and  $6.4 \times 10^5 \text{ s}^{-1}$ . It demonstrates that our model is better than the others in the finite strain range of 0.2–0.55 (the prediction error is less than 10% in the range of 0.3–0.6). In the regimes of strain below 0.3 and greater than 0.6, the error gets bigger. It seems that all these constitutive models including our model will not be satisfactory at very high strain rates.

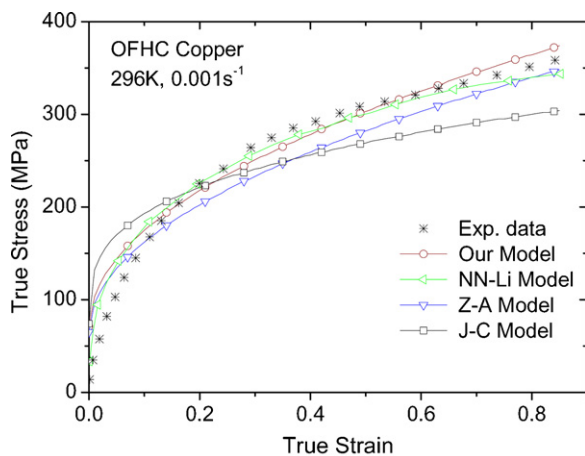


Fig. 3. Comparison of the predictions of various models with experimental data [8] for annealed OFHC copper at 296 K with the strain rate of 0.001/s.

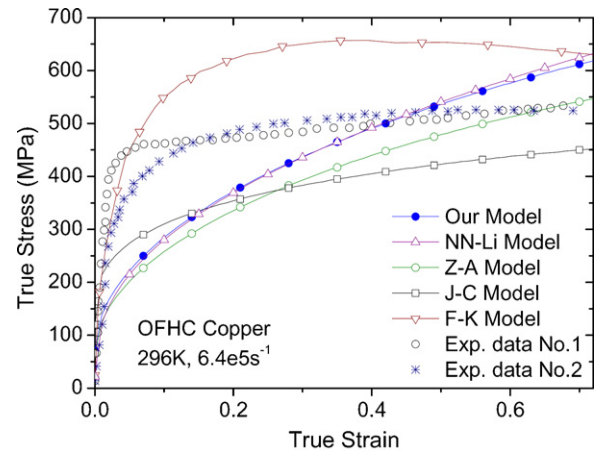


Fig. 4. Comparison of the predictions of various models with experimental data [11] for annealed OFHC copper at room temperature with the strain rate of  $6.4 \times 10^5 \text{ s}^{-1}$ .

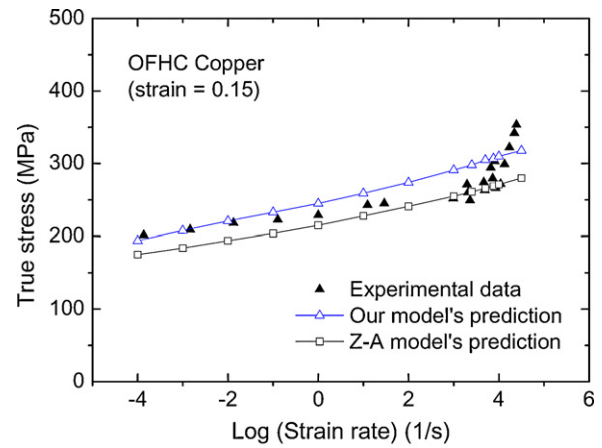


Fig. 5. Relations of flow stress and strain rate and comparison with experimental data [11] for annealed OFHC copper at room temperature with the strain of 0.15.

The results shown in Fig. 5 demonstrate the likely upper boundary of the applicable strain rate range of our model. The comparison of the model predictions with the experimental measurements of the stresses in terms of strain rates (annealed OFHC copper at room temperature with the strain of 0.15) reveals that our model is applicable to a wide range of strain rate up to  $10^4 \text{ s}^{-1}$ . Beyond this rate, there is a strong upturn of the flow stress of OFHC copper, according to the experimental observation in [11], showing an enhanced strain rate sensitivity of the flow stress. It is possible that a new mechanism additional to the thermal activation and dislocation-drag mechanisms, such as an enhanced growth rate of dislocation generation, has become more important beyond this critical strain rate [26].

## 5. Conclusions

Based on the concept of thermal activation mechanism of dislocation motion, this paper has developed a new, simple constitutive model to describe the behavior of FCC metals. The results have shown that the model has a better prediction accuracy compared with the existing ones in the literature in a wide range of strain rate, temperature and strain. Compared with the MTS model, the new model is more concise and becomes explicit, which enables it to be embedded more easily with a computational code of material dynamics. Compared with the Zerilli–Armstrong and J–C models, the model predicts much more accurately. It was also found that

the new model is applicable to a broad range of temperature variation from 77 K to 1096 K, strain rates from  $10^{-3} \text{ s}^{-1}$  to  $10^4 \text{ s}^{-1}$ , and strain close to 1.0.

### Acknowledgments

This research is supported by the Key Project of the National Natural Science Foundation of China under Grant No. 50890174, and the Australian Research Council (ARC) through its discovery project program. The first author thanks Dr. M.C. Cai for his initial help in programming the optimization code of determining constitutive parameters.

### References

- [1] G. Johnson, W. Cook, *Eng. Fract. Mech.* 21 (1985) 31–48.
- [2] J.A. Arsecularatne, L.C. Zhang, *Key Eng. Mater.* 274–276 (2004) 277–282.
- [3] J.D. Campbell, J. Harding, in: P.G. Shewmon, V.F. Zachay (Eds.), *Response of Metals to High Velocity Deformation*, Interscience, New York, 1961, p. 51.
- [4] H.J. Frost, M.F. Ashby, *Deformation Mechanism Maps*, Pergamon Press, Oxford, 1982.
- [5] F.J. Zerilli, R.W. Armstrong, *J. Appl. Phys.* 5 (1987) 1816–1825.
- [6] G.Z. Voyiadjis, F.H. Abed, *Mech. Mater.* 37 (2005) 355–378.
- [7] F.H. Abed, G.Z. Voyiadjis, *Acta Mech.* 175 (2005) 1–18.
- [8] S. Nemat-Nasser, Y.L. Li, *Acta Mater.* 46 (1998) 565–577.
- [9] S. Nemat-Nasser, W. Guo, J. Cheng, *Acta Mater.* 47 (1999) 3705–3720.
- [10] S. Nemat-Nasser, W. Guo, D. Kihl, *J. Mech. Phys. Solids* 49 (2001) 1823–1846.
- [11] P.S. Follansbee, U.F. Kocks, *Acta Metall.* 36 (1988) 81–93.
- [12] P.S. Follansbee, G.T. Gray, *Mater. Sci. Eng. A* 138 (1991) 23–31.
- [13] U.F. Kocks, *Mater. Sci. Eng. A* 317 (2001) 181–187.
- [14] M.A. Meyers, D.J. Benson, O. Vohringer, et al., *Mater. Sci. Eng. A* 322 (2002) 194–216.
- [15] J.R. Klepaczko, *Nucl. Eng. Des.* 127 (1991) 103–115.
- [16] W.S. Lee, C.Y. Liu, *Mater. Sci. Eng. A* 426 (2006) 101–113.
- [17] N.N. Du, A.F. Bower, P.E. Krajewski, et al., *Mater. Sci. Eng. A* 494 (2008) 86–91.
- [18] W.S. Lee, C.F. Lin, *Mater. Sci. Eng. A* 308 (2001) 124–135.
- [19] X.Y. Liu, Q.L. Pan, Y.B. He, et al., *Mater. Sci. Eng. A* 500 (2009) 150–154.
- [20] D.J. Benson, H.H. Fu, M.A. Meyers, *Mater. Sci. Eng. A* 319–321 (2001) 854–861.
- [21] H.S. Kim, Y. Estrin, M.B. Bush, *Mater. Sci. Eng. A* 316 (2001) 195–199.
- [22] L. Lu, M. Dao, T. Zhu, J. Li, *Scripta Mater.* 60 (2009) 1062–1066.
- [23] E. Orowan, *Proc. Phys. Soc.* 52 (1940) 8–22.
- [24] W.G. Johnston, J.J. Gilman, *J. Appl. Phys.* 30 (1959) 129–144.
- [25] U.F. Kocks, A.S. Argon, M.F. Ashby, *Thermodynamics and kinetics of slip*, in: *Progress in Materials Science*, vol. 19, Pergamon Press, 1975.
- [26] R.B. Clough, S.C. Webb, R.W. Armstrong, *Mater. Sci. Eng. A* 360 (2003) 396–407.
- [27] E.A. Davis, *J. Appl. Mech. Trans. ASME* 12 (1945) 13–24.
- [28] M.A. Meyers, *Dynamic Behavior of Materials*, Wiley, New York, 1994.
- [29] O. Yeniay, *Math. Problems Eng.* 2 (2005) 165–173.